

Compact x-ray microscope for the water window based on a high brightness laser plasma source

H. Legall,^{1,2,*} G. Blobel,^{1,2} H. Stiel,^{1,2} W. Sandner,^{1,2} C. Seim,^{3,4}
P. Takman,⁵ D. H. Martz,⁵ M. Selin,⁵ U. Vogt,⁵ H. M. Hertz,⁵ D. Esser,⁶
H. Sipma,⁶ J. Luttmann,⁶ M. Höfer,⁶ H. D. Hoffmann,⁶ S. Yulin,⁷
T. Feigl,⁷ S. Rehbein,⁸ P. Guttmann,⁸ G. Schneider,⁸ U. Wiesemann,⁹
M. Wirtz,⁹ and W. Diete⁹

¹Max-Born-Institut, Max-Born-Str. 2A, D-12489 Berlin, Germany

²Secondary address: BLiX, Hardenbergstr. 36, D-10623 Berlin, Germany

³Technical University Berlin, Institut für Optik und Atomare Physik, Hardenbergstr. 36, D-10623 Berlin, Germany

⁴Secondary address: BLiX, Hardenbergstr. 36, D-10623 Berlin, Germany

⁵Royal Institute of Technology (KTH/Albanova), Biomedical and X-Ray Physics, Roslagstullsbacken 21, SE-10691 Stockholm, Sweden

⁶Fraunhofer-Institut für Lasertechnik ILT, Steinbachstr. 15, D-52074 Aachen, Germany

⁷Fraunhofer-Institut für Angewandte Optik und Feinmechanik IOF, Beutenberg Campus Albert-Einstein-Str. 7, D-07745 Jena, Germany

⁸Helmholtz-Zentrum Berlin für Materialien und Energie GmbH, Institute for Soft Matter and Functional Materials, Albert-Einstein-Str. 15, D-12489 Berlin, Germany

⁹Bruker ASC GmbH, Waltherstrasse 49-51, D-51069 Köln, Germany

*legall@mbi-berlin.de

Abstract: We present a laser plasma based x-ray microscope for the water window employing a high-average power laser system for plasma generation. At 90 W laser power a brightness of 7.4×10^{11} photons/(s x sr x μm^2) was measured for the nitrogen Ly α line emission at 2.478 nm. Using a multilayer condenser mirror with 0.3 % reflectivity 10^6 photons/($\mu\text{m}^2 \times \text{s}$) were obtained in the object plane. Microscopy performed at a laser power of 60 W resolves 40 nm lines with an exposure time of 60 s. The exposure time can be further reduced to 20 s by the use of new multilayer condenser optics and operating the laser at its full power of 130 W.

© 2012 Optical Society of America

OCIS codes: (180.7460) X-ray microscopy; (260.6048) Soft x-rays; (340.7440) X-ray imaging; (350.5400) Plasmas.

References and links

1. J. Kirz, C. Jacobsen, and M. Howells, "Soft x-ray microscopy and their biological applications," *Q. Rev. Biophys.* **28**, 33–130 (1995).
2. G. Schneider, "Cryo X-ray microscopy with high spatial resolution in amplitude and phase contrast," *Ultramicroscopy* **75**, 85–104 (1998).
3. D. Weiss, G. Schneider, B. Niemann, P. Guttmann, D. Rudolph, G. Schmahl, "Computed tomography of cryogenic biological specimens based on X-ray microscopic images," *Ultramicroscopy* **84**, 3–4 (2000).
4. G. Schneider, P. Guttmann, S. Heim, S. Rehbein, F. Mueller, K. Nagashima, J. B. Heymann, W. G. Miller, and J. G. McNally, "Three-dimensional cellular ultrastructure resolved by X-ray microscopy," *Nat. Meth.* **7**, 985–987 (2010).
5. C. A. Larabell and K. A. Nugent, "Imaging cellular architecture with X-rays," *Curr. Opin. Struct. Biol.* **20**, 623–631 (2010).

6. G. Schneider, P. Guttman, S. Rehbein, S. Werner, and R. Follath, "Cryo X-ray microscope with flat sample geometry for correlative fluorescence and nanoscale tomographic imaging," *J. Struct. Biol.* **177**, 212–223 (2012).
7. S. Rehbein, P. Guttman, S. Werner, and G. Schneider, "Characterization of the resolving power and contrast transfer function of a transmission X-ray microscope with partially coherent illumination," *Opt. Express* **20**, 5830–5839 (2012).
8. W. Chao, P. Fischer, T. Tyliczszak, S. Rekawa, E. Anderson, and P. Naulleau, "Real space soft x-ray imaging at 10 nm spatial resolution," *Opt. Express* **20**, 9777–9783 (2012).
9. M. Berglund, L. Rymell, M. Peuker, T. Wilhein, and H. M. Hertz, "Compact water-window transmission microscopy," *J. Microscopy* **197**, 268–273 (2000).
10. P. A. C. Jansson, U. Vogt, and H. M. Hertz, "Liquid-nitrogen-jet laser-plasma source for compact soft x-ray microscopy," *Rev. Sci. Instrum.* **76**, 435031 (2005).
11. P. A. C. Takman, H. Stollberg, G. A. Johansson, A. Holmberg, M. Lindblom, and H. M. Hertz "High-resolution compact X-ray microscopy," *J. Microsc.* **226**, 175–181 (2007).
12. H. M. Hertz, O. von Hofsten, M. Bertilson, U. Vogt, A. Holmberg, J. Reinsprach, D. Martz, M. Selin, A. E. Christakou, J. Jerlström-Hultqvist, and S. Svård "Laboratory cryo soft X-ray microscopy," *J. Struct. Biol.* **177**, 267–272 (2012).
13. M. Bertilson, O. von Hofsten, U. Vogt, A. Holmberg, A. E. Christakou, and H. M. Hertz, "Laboratory soft x-ray microscope for cryotomography of biological specimens," *Opt. Lett.* **36**, 2728–2730 (2011).
14. K. W. Kim, Y. Kwon, K.-Y. Nam, J.-H. Lim, K.-G. Kim, K. S. Chon, B. H. Kim, D. E. Kim, J. G. Kim, B. N. Ahn, H. J. Shin, S. Rah, K.-H. Kim, J. S. Chae, D. G. Gweon, D. W. Kang, S. H. Kang, J. Y. Min, K.-S. Choi, S. E. Yoon, E.-A. Kim, Y. Namba, and K.-H. Yoon, "Compact soft x-ray transmission microscopy with sub-50 nm spatial resolution," *Phys. Med. Biol.* **31**, N99–107 (2006).
15. M. Benk, K. Bergmann, D. Schaefer, and T. Wilhein, "Compact soft x-ray microscope using a gas-discharge light source," *Opt. Lett.* **33**, 2359–2361 (2008).
16. M. Benk, D. Schäfer, T. Wilhein, and K. Bergmann, "High power soft x-ray source based on a discharge plasma," *Journal of Physics: Conference Series (IOP), Proc. of the 9th International Conference on x-ray Microscopy* **186**, 012024–1–3 (2009).
17. T. Wilhein, D. Hambach, B. Niemann, M. Berglund, L. Rymell, and H. M. Hertz, "Off-axis reflection zone plate for quantitative soft x-ray source characterization," *Appl. Phys. Lett.* **71**, 190–192 (1997).
18. J. Thieme, "Theoretical investigations of imaging properties of zone plates and zone plate systems using diffraction theory," in *X-ray Microscopy II*, D. Sayre, M. R. Howells, J. Kirz, H. Rarback, eds. (Springer Series in Optical Sciences **56**, Springer, Berlin, 1988), pp 70–79.
19. M. Bertilson, O. von Hofsten, U. Vogt, A. Holmberg, and H. M. Hertz, "High-resolution computed tomography with a compact soft x-ray microscope," *Opt. Express* **17**, 11057–11065 (2009).
20. J.-F. Adam, J.-P. Moy, and Susini, "Table-top water window transmission x-ray microscopy: review of the key issues, and conceptual design of an instrument for biology," *Rev. Sci. Instrum.* **76**, 1–14 (2005).
21. P. Loosen, M. Höfer, D. Esser, H. Sipma, R. Kasemann, and H. D. Hoffmann, "Advanced INNOSLAB Solid-state-lasers for the generation of bright XUV/EUV-radiation," *Proc. International Workshop on EUV and Soft X-ray Sources 2010* <http://www.euvlitho.com/2010/P37.pdf>.
22. T. Wilhein, S. Rehbein, D. Hambach, M. Berglund, L. Rymell, and H. M. Hertz, "A slit grating spectrograph for quantitative soft x-ray spectroscopy," *Rev. Sci. Instrum.* **70**, 1694–1699 (1999).

1. Introduction

Soft x-ray microscopy in the spectral range of the water window between 2.3 and 4.4 nm is ideally suited for the investigation of carbon containing structures in wet or frozen samples [1]. The high contrast between carbon and oxygen in this spectral range facilitates investigations of "thick" biological specimens in its natural environment. The highest transparency of radiation through water is obtained in this spectral range close to the absorption edge of oxygen. Near this edge the 1/e penetration depth of radiation in water is 10 μm . Cryogenic (quick frozen) samples can withstand high radiation dose without visible change in their structure [2]. Thus, 3-dimensional high resolution microscopy is feasible [3]. This opportunity makes water window microscopy attractive for cell biology studies and other applications in life science. Conventionally, micro zone plate based soft x-ray microscopes for investigations of 3-dimensional structures of biological specimens with nanometer resolution are operated with bright synchrotron radiation sources [4, 5].

Full-field X-ray microscopes with zone plate objectives installed at electron storage rings use bending magnets or undulators as x-ray sources. Bending magnets provide a total photon flux

of about 10^{12} photons/(s 100mA in 0.1%BW) illuminating a condenser zone plate of 9 mm diameter. In combination with the zone plate condenser a spectral resolution of about $\lambda/\Delta\lambda = 500$ is achieved. Assuming an efficiency of 8% for the diffractive condenser, and including two vacuum windows the total photon flux is about 8×10^{10} photons/(s 100mA in 0.2%BW) onto the sample. An image field of $15 \times 15 \mu\text{m}^2$ is illuminated with a photon density of 3×10^8 photons/(s μm^2 100mA in 0.2%BW). An X-ray microscope at an undulator starts with two orders of magnitude higher photon flux from the source. The only worldwide existing soft X-ray full-field microscope at an undulator beamline at BESSY II in Berlin employs a spherical grating monochromator beamline to illuminate an elliptically shaped mirror as condenser. With this setup the spectral resolution is $\lambda/\Delta\lambda = 10.000$ and the condenser efficiency is 80% [6]. The photon density illuminating the sample is about 7×10^8 photons/(s μm^2 100mA in 0.01%BW) for the undulator based TXM under these conditions. Note that the undulator TXM operates at an order of magnitude better spectral resolution with similar photon densities than the bending magnet TXM. Overall, both microscopes at bending magnet or undulator sources provide exposure times on the order of 1 s for imaging at 25 nm resolution (half-pitch). The spatial resolution record values are 10 nm (half-pitch) [7, 8].

In the last decades the laboratory water window x-ray microscopy has made significant progress [9–12]. Presently a handful of high resolution zone plate based laboratory x-ray microscopes in the water window are in operation worldwide [13–15]. It is remarkable that these laboratory microscopes for the water window are exclusively based on plasma sources. Plasma sources using nitrogen as target are particularly suited for laboratory water window x-ray microscopy at the short wavelength edge of the water window, because of a strong hydrogenlike and heliumlike nitrogen ion line emission at 2.478 nm and 2.879 nm. While with high repetition discharge gas plasma sources the He_α emission line clearly dominates the spectrum [15, 16], with high repetition laser plasma sources the hydrogenlike Ly_α line emission at 2.478 nm can be generated more efficiently. The line width of the Ly-alpha line was determined to be ≈ 2 pm [17], which gives a $\lambda/\Delta\lambda \approx 1000$. This monochromaticity is sufficient to avoid chromatic aberration in zone plate imaging with state-of-the-art zone plates, since the $\Delta\lambda/\lambda$ for achievement of the diffraction-limited resolution should vary like $1/N$ [18], where N is the number of zones. In contrast to gas discharge sources, for the laser plasma x-ray generation in the water window dense liquid nitrogen jet target systems are used. The use of a liquid nitrogen jet target enables stable plasma operation at high repetition rates with low debris emission and high brightness due to a small source size. The brightness, defined as photons/(s x sr x μm^2 in line), is the most important source criteria of a laboratory x-ray microscope since it directly translates into sample illumination, given that all other parameters are equal. The small source size of laser plasmas, typically a few tens of microns, is furthermore advantageous in order to reduce the influence of stray light in the images [19]. The source size of a high power discharge plasma source is in the range of about 1 mm and hence much larger than that of the laser plasma source. A brightness of 4.3×10^9 photons/(s x sr x μm^2 in He_β line) has been demonstrated [15] for discharge laser plasma sources. For laser plasma sources a brightness of 4.1×10^{10} photons/(s x sr x μm^2 in Ly_α line) is presently reported in literature [10, 11].

In this work, we present a novel table top x-ray microscope for the water window based on a compact highly brilliant laser plasma source pumped by a kHz laser system. It will be shown that the acquisition time for an image with a laboratory microscopy setup can be reduced to several seconds. Hence routine 3-dimensional microscopy becomes available in the laboratory. This could pave the way for a more extensive use of water window microscopy by scientists from biology and medicine [20]. The characteristic parameters of the laboratory setup are shown and the performance of the table top x-ray microscope in the water window is demonstrated.

2. Experimental arrangement

The arrangement of the microscope is shown in Fig. 1. The plasma is generated by focusing a pulsed laser beam on a target surface. For the laser plasma source a liquid nitrogen cryo jet target is used. A detailed description of the used liquid nitrogen target system developed at KTH Stockholm can be found in [10]. The laser for plasma generation is a MOPA (Master Oscillator Power-Amplifier) system consisting of a diode seeded regenerative amplifier and a chain of three INNOSLAB power amplifier stages, developed by ILT Aachen [21]. Laser pulses with a duration of 450 ps (accessible range: 0.25 - 1.5 ns) are amplified up to a stable average power of 130 W at a repetition rate of 1.3 kHz and a laser emission wavelength of 1064 nm. The slab crystals are end pumped by diode laser stacks. The slow axis of the stacks is oriented horizontally and homogenized by a waveguide. Hence the horizontal direction of the beam is referred to as “slow axis” and the vertical direction as “fast axis”. The laser beam was characterized using a beam propagation analyzer (Spiricon M2-200s). Using the 90/10 knife edge method a beam quality factor of about $M^2_{slow} \approx 3$ was measured in the slow axis. In the fast axis the beam is nearly diffraction limited $M^2_{fast} \approx 1$. A shaping of the slow beam axis is performed to adapt the beam size and divergency in both axes. After shaping, the beam is expanded by a telescope before it is focused by a lens triplet into the plasma chamber. The focusing lenses are placed outside the plasma chamber to prevent debris contamination. The focal length of the lens triplet is 135 mm. Behind the focusing lenses 92 % of the laser output power was detected. A focus size of $20 \times 24 \mu\text{m}$ ($10.5 \times 11.6 \mu\text{m}$ (FWHM) for the central spot in Fig. 2) was measured with the 90/10 knife edge method using a laser beam analyzer (Spiricon LBA-FW-SCOR). After rotation of the beam by 90 degree about 83 % of the laser output energy hits the surface of the cryo jet target.

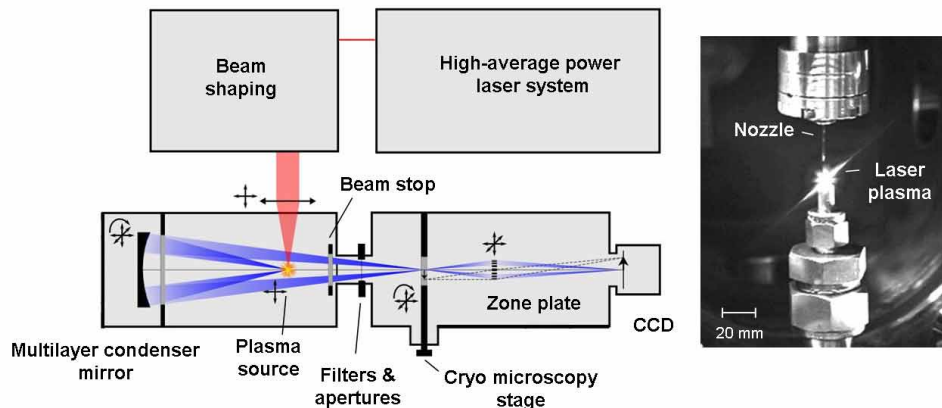


Fig. 1. The arrangement and optical layout of the table top water window x-ray microscope.

Emission spectra and the emitted photon flux of the laser plasma source were measured using a calibrated (PTB at BESSY II) transmission grating spectrograph (TGS) [22]. The transmission grating is a gold coated quasi freestanding silicon line structure with 10 000 lines/mm. A slit with a size of 0.05×1 mm was placed directly in front of the grating. The source to grating distance was 1060 mm. A calibrated 200 nm thick mesh supported Cr filter ($T = 0.48$ at 2.478 nm) was placed in front of the slit-grating arrangement in order to avoid that scattered laser light illuminates a cooled 16-bit thinned back-illuminated CCD camera. The CCD camera was positioned in a distance of 400 mm behind the grating. The emission spectra were recorded in first order of diffraction. The exposure time of the CCD was controlled by a fast

bistable shutter placed at the exit flange of the plasma chamber. Measurements of the plasma source size were performed with the spherical multilayer at 2.478 nm by imaging the plasma source on a CCD camera.

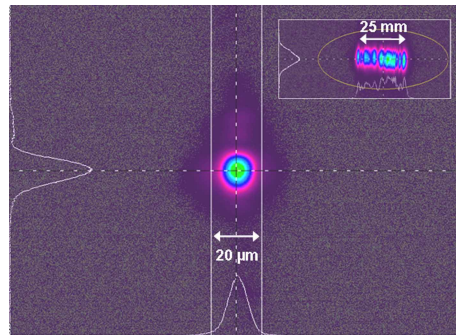


Fig. 2. Laser beam in the focus. The lines indicate the dimensions of the liquid nitrogen jet. The beam profile at the laser exit is also shown. The beam in the focus image is rotated by 90 degree to the beam at the laser output.

For sample illumination in the microscope a spherical Cr/V multilayer condenser mirror (FhG-IOF Jena) is used in normal incidence geometry. The usable radial aperture is 54 mm in diameter, the radius of curvature is 350 mm. The bandwidth at 2.478 nm is 0.008 nm (FWHM) with a peak reflectivity up to 0.4 %. The mirror was placed in a distance of 264 mm to the laser plasma source. In this distance, radiation reflected over a mirror diameter of 52 mm matches the numerical aperture $NA = 0.05$ of the zone plate with an outermost zone width of 25 nm. A central beam stop is placed between source and sample at the exit of the plasma source unit. It blocks the radiation emitted by the source into the direction of the sample and forms a hollow cone illumination. Scattered laser radiation was suppressed in front of the sample by placing a 200 nm Al filter and apertures behind the exit flange. The plasma source is imaged with a magnification factor of 2:1 onto the sample plane. The microscope image was recorded by a back illuminated 16-bit XUV CCD (model: PI-SX NTE 2048 x 2048) with a pixel size of $13.5 \mu\text{m}$. Zone plate and sample positioning are integrated in a compact microscopy unit of Bruker ASC. The microscopy unit enables a quick transfer of samples into vacuum with a load lock. The accuracy of sample positioning is $< 0.1 \mu\text{m}$ for linear positioning and $< 1^\circ$ for angle adjustments. The zone plate is positioned with a piezo driven three-axis stage. Cryo tomography of quick-frozen samples can be performed with the microscopy unit using a cryo sample holder (Gatan Inc., model: 626).

3. Results and discussion

Emission spectra of the liquid nitrogen plasma emission obtained for different laser pulse energies are depicted in Fig. 3. The acquisition time per spectrum was 5 s. The overall intensity as well as the relative intensities of the displayed hydrogenlike and heliumlike nitrogen emission lines, which reflects the plasma temperature, depend on laser pulse energy. Fluctuations in the photon flux emitted by the plasma source were determined to be $< 15\%$ for sequentially performed measurements. The spatial stability of the laser plasma source is about $\pm 5 \mu\text{m}$ (peak-to-valley).

The photon flux in the emission lines was estimated by integrating over twice the FWHM of the emission lines. The results are summarized in Table 1. The maximum photon flux per pulse in Table 1 was obtained at a laser output power of 90 W (69 mJ/pulse) with a laser pulse energy

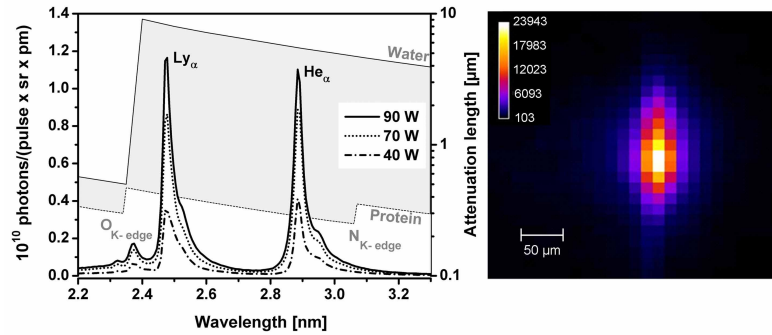


Fig. 3. On the left: Emission spectra of the liquid-nitrogen plasma. On the right: Measured x-ray beam size in the focus of the condenser multilayer mirror at a laser power of 60 W (the pixel size is $13.5 \mu\text{m}$, two $2 \mu\text{m}$ Al filters were additionally placed in front of the CCD).

of 58 mJ on the target. The maximum photon flux at 2.478 nm in Table 1 corresponds to an averaged photon flux of 6×10^{14} photons/(s x sr x line). The corresponding photon flux at 60W laser power used for microscopy in this paper is 3.2×10^{14} photons/(s x sr x line).

Table 1. X-ray flux of the nitrogen plasma emission lines measured with a laser pulse width of 450 ps at a laser wavelength of 1064 nm. The conversion efficiency (CE) in brackets is calculated for isotropic emission in 4π . The pulse energy is measured on the target.

P_{laser} (W)	E_{pulse} (mJ)	I_{focus} (W/cm ²)	$\lambda = 2.478 \text{ nm}$		$\lambda = 2.879 \text{ nm}$	
			ph/(pulse sr line) (CE% in 4π)		ph/(pulse sr line) (CE% in 4π)	
40	26	5.3×10^{13}	1.6×10^{11} (0.61)		2.0×10^{11} (0.66)	
70	46	9.3×10^{13}	3.0×10^{11} (0.67)		4.2×10^{11} (0.79)	
90	58	1.2×10^{14}	4.6×10^{11} (0.79)		5.8×10^{11} (0.86)	

The source size at 2.478 nm was determined by imaging the source with the multilayer mirror onto the CCD camera. In Fig. 3 the magnified image of the plasma source is shown. The image of the source is elliptically shaped with a size of $36 \times 90 \mu\text{m}^2$ (FWHM). If the magnification factor in the used multilayer condenser geometry of 2:1 is taken into consideration, the plasma source size can be calculated to $18 \times 45 \mu\text{m}^2$. This gives a brightness of the laser plasma source of 7.4×10^{11} photons/(s x sr x μm^2 in Ly_α line) at a laser power of 90 W.

The reflectivity of the multilayer condenser mirror was determined at different radial positions on the mirror for an incidence angle of $\Theta = 2^\circ$ by the PTB at BESSY II (Fig. 4). For the angles of incidence in the microscope setup between 0.5° and 1.5° the reflectivity of the multilayer mirror in Fig. 4 matches the emission wavelength of the plasma source at 2.478 nm. Calculations yield a reflectivity, averaged over the multilayer mirror diameter, of about 0.34 % in the used optical geometry. Here it was assumed that only the Ly_α line with a width of some pm [17] is reflected. The reflected radiation collected by the CCD behind the focus position without zone plate is shown in Fig. 4. Integrating the photon flux over the illuminated area in Fig. 4 gives a measured integral reflectivity of the multilayer of about 0.3 %, which is very close to the expected reflectivity.

The microscopy experiments presented in this article were performed at 60 W laser power. The latter was a consequence of a degradation of the laser pump diodes. At a laser power of 60 W the measured averaged intensity in the sample plane (integrated over 9 pixel in square on the

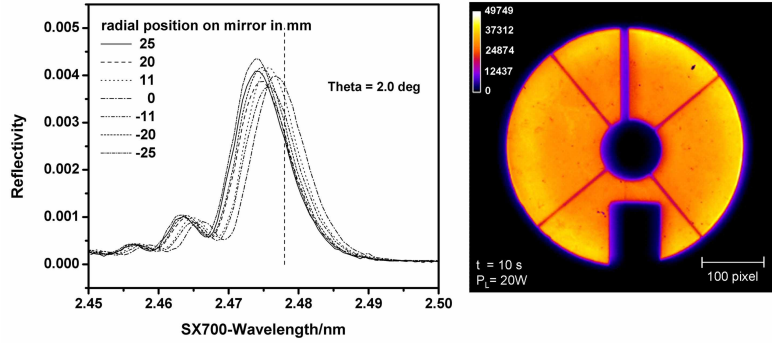


Fig. 4. On the left: Reflectivity measurements of the multilayer condenser mirrors fabricated by IOF FhG after annealing. The measurements were performed by Physikalisch Technische Bundesanstalt (PTB). On the right: Image of the multilayer reflection recorded behind the focus of the multilayer condenser mirror. The image was collected at 20 W laser power. A $2 \mu\text{m}$ Al filter was additionally placed in front of the CCD camera.

CCD in Fig. 4) is 5.4×10^5 photons/(s $\times \mu\text{m}^2$). About 10^6 photons/($\mu\text{m}^2 \times \text{s}$) were measured in 1 pixel at 70 W. For x-ray imaging a micro zone plate with 25 nm outermost zone width was used. In Fig. 5 x-ray images of dried diatoms on a 200 nm thick Si_3Ni_4 ($T = 0.39$) membrane and zone plate images recorded at 60 W laser power are shown. The images of the diatoms were recorded in 2 min and the zone plate image in Fig. 5(c) in 3 min with a pixel size of 26 nm in the object plane. The zone plate image in Fig. 5(d) was collected in 1 min with a pixel size of 13.5 nm in the object plane. The half-pitch resolution derived from these images is about 50 nm for the images 5(a)–5(c) and 40 nm for the image shown in Fig. 5(d). Without sample the detector is illuminated at 60 W with averaged 12 ± 2 ph/s per 26 nm pixel. These photon numbers per pixel indicate a zone plate diffraction efficiency of about 5 %.

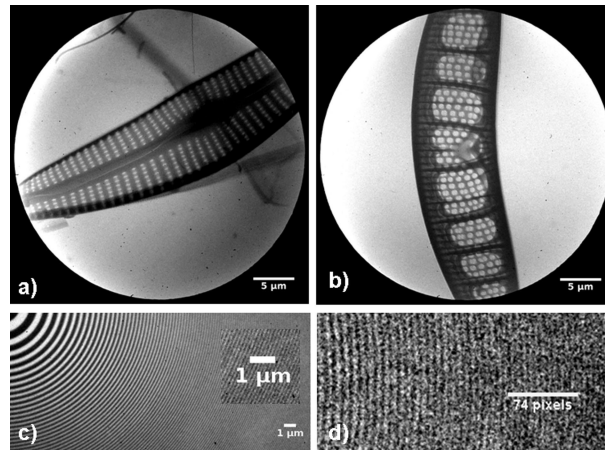


Fig. 5. Microscope images of diatoms and zone plate structures. The images (a)–(c) were taken with a pixel size of 26 nm, the image (d) with a pixel size of 13.5 nm. The exposure times were 2 min for image (a) and (b), 3 min for (c) and 1 min for image (d).

4. Conclusions and future directions

We have shown that high-quality water-window microscopy images can be recorded with attractive exposure times in a table-top arrangement based on a high-average power laser-plasma source. The measured intensity in the sample plane at 2.478 nm was increased by a factor 5-10 in comparison to the laboratory microscope arrangements reported in [10, 11]. In the near future the exposure times will be further reduced by a factor three. The laser system will be refurbished so that it again reaches 130 W (100 mJ/pulse), which is more than a factor two higher than the 60 W used for microscopy in the present paper. A further reduction of recording times is already available by using a new multilayer condenser mirror with 0.6 % peak reflectivity. These two improvements would allow to record the images in Fig. 5 in < 20 s.

Acknowledgments

This project was funded by the BMBF (#13N8913) and the BMVBS (WTW #03WWBE106).